

Inherent Global Stabilization of Unstable Local Behavior in Coupled Map Lattices

Harald Atmanspacher^{1,2} and Herbert Scheingraber¹

1 Center for Interdisciplinary Plasma Science,
Max-Planck-Institut für extraterrestrische Physik,
85740 Garching, Germany

2 Institute for Frontier Areas of Psychology and Mental Health,
Wilhelmstr. 3a, 79098 Freiburg, Germany

Accepted for publication in
Intern. Journal of Bifurcation and Chaos

Abstract

The behavior of two-dimensional coupled map lattices is studied with respect to the global stabilization of unstable local fixed points without external control. It is numerically shown under which circumstances such inherent global stabilization can be achieved for both synchronous and asynchronous updating. Two necessary conditions for inherent global stabilization are derived analytically.

1 Introduction

Coupled map lattices (CMLs) are arrays of states whose value is continuous, usually within the unit interval, over discrete space and time. Starting with Turing's seminal work on morphogenesis [Turing 1952], they have been used to study the behavior of complex spatiotemporal systems for 50 years. More recently, Kaneko and collaborators have established many interesting results for CMLs (cf. Kaneko [1993]) as generalizations of cellular automata, whose state values are discrete.

One key motivation for modeling spatiotemporally extended systems with CMLs is to simplify the standard approach in terms of partial differential equations. And, of course, CMLs would not have become accessible without the rapid development of fast computers with large storage capacities. Within the last decades, CMLs have been applied to the study of areas as diverse as social systems, ecosystems, neural networks, spin lattices, Josephson junctions, multimode lasers, hydrodynamical turbulence, and others (cf. the special journal issues *CHAOS* **2**(3), 1992, and *Physica D* **103**, 1997).

A compact characterization of a CML over two spatial dimensions with one time parameter is given by:

$$g_{n+1}(x_{ij}) = (1 - \epsilon)f_n(x_{ij}) + \frac{\epsilon}{N} \sum_{k=1}^N f_n(x_k) \quad (1)$$

For $f_n(x)$, the iterative logistic map $x_n = rx_{n-1}(1 - x_{n-1})$ is mostly used, where r is a control parameter, $0 < r \leq 4$, and n represents the time step of the iteration. The indices i, j are used to label the position of each cell (or site) in the lattice. N is the number of cells defining the neighborhood of each cell (with periodic boundary conditions), and k runs over all neighboring cells. The parameter ϵ specifies the coupling between each cell and its neighborhood (and is usually considered as constant over time and space). Thus, the value of $g_{n+1}(x_{ij})$ is a convex combination of the value at each individual cell and the mean value of its local neighborhood.

For $\epsilon \rightarrow 0$, there is no coupling at all; hence, local neighborhoods have no influence on the behavior of the CML. This situation represents the limiting case of N_{tot} independently operating local objects at each lattice site. In the general case $0 < \epsilon < 1$, the independence of individual cells is lost and the lattice behavior is governed by both local and global influences. CMLs with a maximal neighborhood, $N \approx N_{tot}$, are often denoted as globally coupled maps. If the coupling is maximal, $\epsilon \rightarrow 1$, the behavior of the entire CML is determined by global properties alone (mean field approach).

The second term on the rhs in Eq. (1) contains the states of the neighboring map sites at the same time step n at which the first term specifies the state of the site whose neighborhood is considered. This type of coupling, assuming a vanishing transmission time $\Delta t \rightarrow 0$, is sometimes called “future coupling” [Mehta & Sinha 2000] since it refers to a situation in which the neighborhood states are treated as if they act back from future to present. In order to take a finite transmission time

$\Delta t > 0$ into account, one can modify the second term in Eq. (1) such that $f_n(x_k)$ is replaced by $f_{n-1}(x_k) = x_k$. In this way, past states in the neighborhood of a site are considered to act on the present state of a given site with limited signal speed so that interactions are delayed rather than instantaneous. Corresponding coupling scenarios, which have recently been studied by Mehta & Sinha [2000], Masoller et al. [2003], Li et al. [2004], and Atay et al. [2004], will be focused at in the present paper.

Another time scale important for the physical interpretation of Eq. (1) is the time interval $\Delta\tau$ assumed for the updating mechanism, i.e. for the physical integration of signals from the neighborhood states with the state considered. If signals between cells are transmitted much slower than the time scale assumed for the updating mechanism, $\Delta\tau \ll \Delta t$, the updating can be implemented (almost) instantaneously, or synchronously. If this is not the case, $\Delta\tau \gtrsim \Delta t$, updating must be implemented in an asynchronous way. This entails the additional problem of determining a proper updating sequence, which can be random or depend on particular features of the situation considered.

Most of the work on CMLs published in this respect (cf. Kaneko and Tsuda [2000]) was based on synchronous updating. For asynchronous updating as, for instance, studied by Lumer & Nicolis [1994], it was found that the behavior of CMLs differs strongly from that of CMLs with synchronous updating. Additional results for asynchronous updating were reported by Marcq et al. [1997], Rolf et al. [1998], and Mehta & Sinha [2000]. Asynchronous updating rules have been suggested as particularly relevant for neurobiological networks. The relevance of CMLs with functions with quadratic maximum (such as the logistic map) as models for neurobiological networks was recently substantiated by novel results concerning a non-monotonic (rather than sigmoid) transfer function for individual neurons (Kuhn et al. [2004]).

As a common feature of the (so far) few studies of asynchronous updating, it has been reported that it facilitates the synchronization and stabilization of CMLs decisively. In particular, Mehta & Sinha [2000] demonstrated that the dynamics at individual lattice cells is strongly synchronized by coupling among cells. In this contribution we will focus on specific stability properties of CMLs rather than their synchronization and evolving patterns. In particular, we will show that unstable fixed points at individual cells can be stabilized as a consequence of their coupling to neighboring unstable fixed points. (For more general issues concerning the asymptotic stability of densities in coupled map lattices compare Mackey & Milton [1995].)

Such a stabilization is of particular interest since it is independent of external control mechanisms. The global stabilization of unstable local behavior operates inherently, without external adjustment, once the coupling is strong enough. At a speculative level, such a possibility was indicated by Atmanspacher & Wiedenmann [1999]. It represents a powerful alternative to external control procedures in the style of “controlling chaos” (Ott et al. [1992]).

Another motivation to study globally stabilized local instabilities derives from

work on the perception of bistable stimuli in cognitive contexts. Recently, a specific neural correlate in event-related potentials was discovered for the switching process between the two different mental representations of a bistable stimulus (Kornmeier et al. [2004]). As outlined by Atmanspacher [1992], the unstable state between the two (meta-)stable representations might be an interesting candidate for particular stabilization procedures.

The following section 2 presents the results of numerical simulations of CMLs with synchronous and asynchronous updating, for different coupling strengths $0 < \epsilon < 1$, and for different types and sizes of neighborhoods. It will be demonstrated that stabilizing effects for unstable local behavior are generic for asynchronous updating with strong enough coupling. For synchronous updating, it depends on the type of neighborhood whether and when such a stabilizing effect occurs.

In section 3, the stabilizing effect for local unstable behavior is considered from an analytical point of view. It will be shown how the inherent global stabilization of unstable local fixed points can be understood in terms of a “squeeze-and-shift” procedure applied to the logistic map. Two necessary conditions for the stabilization will be derived and significant parameters will be discussed.

Section 4 summarizes and concludes the paper, and some perspectives will be addressed.

2 Numerical Results

In this section, we present results from numerical simulations of two-dimensional coupled map lattices according to Eq. (1). Since the focus of this contribution is on the stabilization of unstable behavior, we have to work within a parameter range in which the behavior of the logistic maps at each lattice site is unstable.

The logistic map $x_n = rx_{n-1}(1 - x_{n-1})$ has two critical points, one at 0 and one at $\frac{r-1}{r}$. The stability properties of these critical points are directly related to the derivative of the function $x \mapsto rx(1 - x)$ at each of them. If the absolute value of the derivative is smaller (greater) than 1, then the critical point is stable (unstable). Hence, the critical point at 0 is a stable fixed point for $r < 1$ and unstable for $r \geq 1$. The critical point at $\frac{r-1}{r}$ is stable for $r < 3$ and unstable for $r \geq 3$.

For our investigations, we focus on the more interesting unstable fixed point at $\frac{r-1}{r}$ and use the control parameter $r = 4$ to demonstrate the results. (As far as the topic of this contribution is concerned, there is no basic difference in behavior for other values of r as long as $r > 3$.) The corresponding unstable fixed point is located at 0.75. We study the distribution of state values of a lattice of size 50×50 ($N_{tot} = 2500$ cells with random initial conditions) after a number of iterations which is large enough that transients have died out, usually after 10000 iteration steps.

We consider different kinds of neighborhoods according to the second term of Eq. (1). Results for both von Neumann neighborhoods and Moore neighborhoods will be presented, each of both order 1 and 2. A von Neumann neighborhood of order 1 includes the $N = 4$ vertically and horizontally nearest neighbors of a given

site. A Moore neighborhood of order 1 includes the 4 diagonal nearest neighbors in addition, hence covering a square of $N = 8$ cells in total. A von Neumann neighborhood of order 2 is constructed by a Moore neighborhood of order 1 plus the vertical and horizontal second neighbors of a given site, hence it consists of $N = 12$ cells in total. A Moore neighborhood of order 2 covers, in addition, all cells covering a square of side length 5, hence $N = 24$ cells in total.

As mentioned in the introduction, the behavior of CMLs depends on the way in which the values at each cell are updated from one to the next iteration step. As two basic types of updating, we distinguish between synchronous updating, where all values are calculated subsequently but updated at once, and asynchronous updating, where all values are updated in the sequence in which they are calculated. For the latter procedure, it is crucial how the sequence is defined. In case of asynchronous updating, those cells which are already updated affect the behavior of the CML before the update providing the next iteration step is complete. This does not happen in case of synchronous updating.

2.1 Synchronous Updating

Figures 1 and 2 show histograms for the distribution of state values at individual cells after 10000 iteration steps for a von Neumann neighborhood of order 1 and a Moore neighborhood of order 1, for coupling strengths $\epsilon = 0.5$ (Figs. 1a, 2a) and $\epsilon = 0.8$ (Figs. 1b, 2b). Figs. 1a and 2a show two differently pronounced peaks right and left of the unstable fixed point at 0.75, indicating oscillatory behavior of the overall state distribution of the CML. (For neighborhoods of order 2, similar behavior is observed.) The situation is different in Figs. 1b and 2b. While the oscillating behavior is maintained for the von Neumann neighborhood of order 1, the Moore neighborhood of order 1 produces a stabilization of the CML at the unstable fixed point at 0.75 at each cell. (Both neighborhoods provide stabilization at 0.75 if they are of order 2.)

Fig. 3 gives an overview representation of this behavior, a so-called stability diagram, for the full range $0 \leq \epsilon \leq 1$. The vertical axis indicates mean values of the state distribution left and right of the unstable fixed point at 0.75, respectively, which are averaged over ten different sets of random initial conditions for the CML. The four curves represent the four different types of neighborhood.

The behavior shown in Figs. 1a,b and 2a,b corresponds to one point for each histogram in the stability diagram Fig. 3. Error bars are of the size of the symbols. It is clearly visible that the von Neumann neighborhood of order 1 does not reach stabilization at 0.75 but stays bimodal until the mean value of the distribution of initial states (≈ 0.5) is obtained for $\epsilon = 1$ (this is the case for all types of neighborhood). For all other types of neighborhood considered, there is a critical value of ϵ at which stabilization sets in. This critical value decreases for an increasing order of the neighborhood (even beyond 2, although this is not shown here). For small values of ϵ , the behavior of all four stability curves is essentially identical.

As a result, local unstable behavior of the logistic map (at the unstable fixed

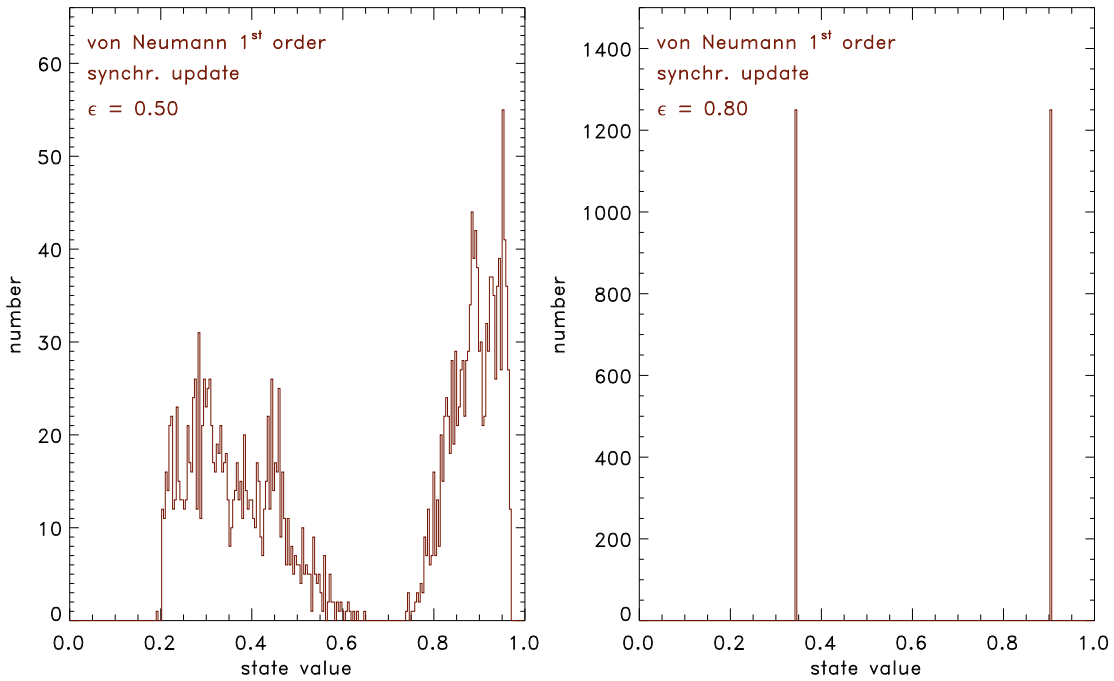


Figure 1: State histograms for synchronously updated CMLs with a von Neumann neighborhood of order 1 for coupling strengths (a) $\epsilon = 0.5$ (left) and (b) $\epsilon = 0.8$ (right). The control parameter of the logistic map is set at $r = 4$, and the number of iterations is 10000.

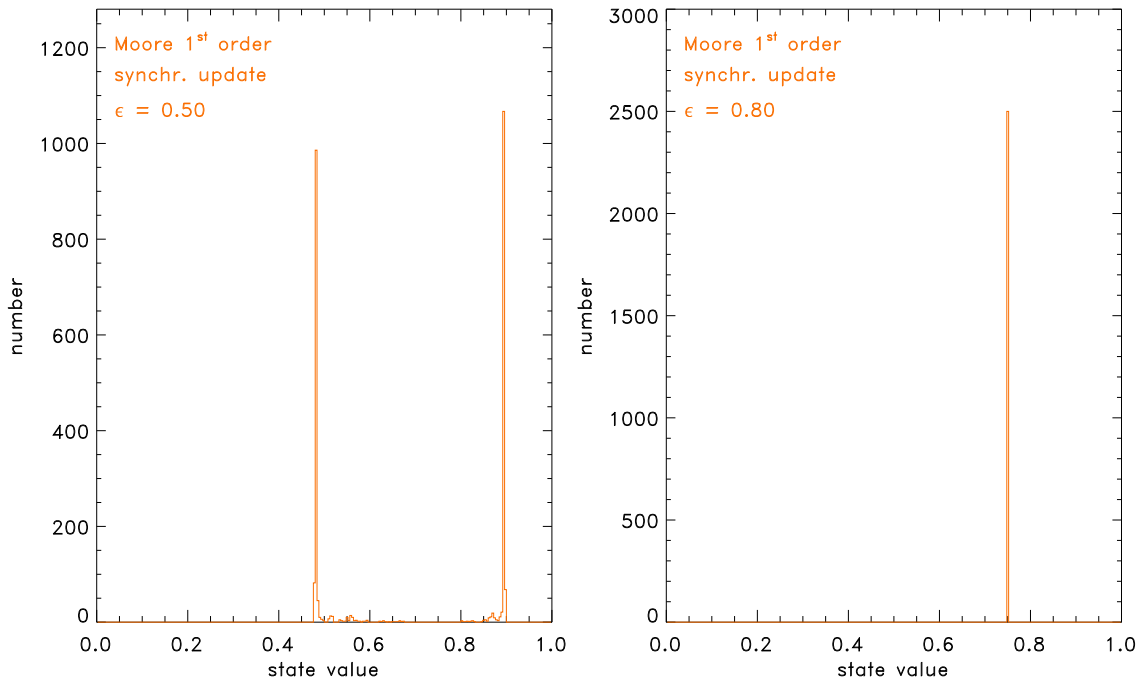


Figure 2: State histograms for synchronously updated CMLs with a Moore neighborhood of order 1 for coupling strengths (a) $\epsilon = 0.5$ (left) and (b) $\epsilon = 0.8$ (right). The control parameter of the logistic map is set at $r = 4$, and the number of iterations is 10000.

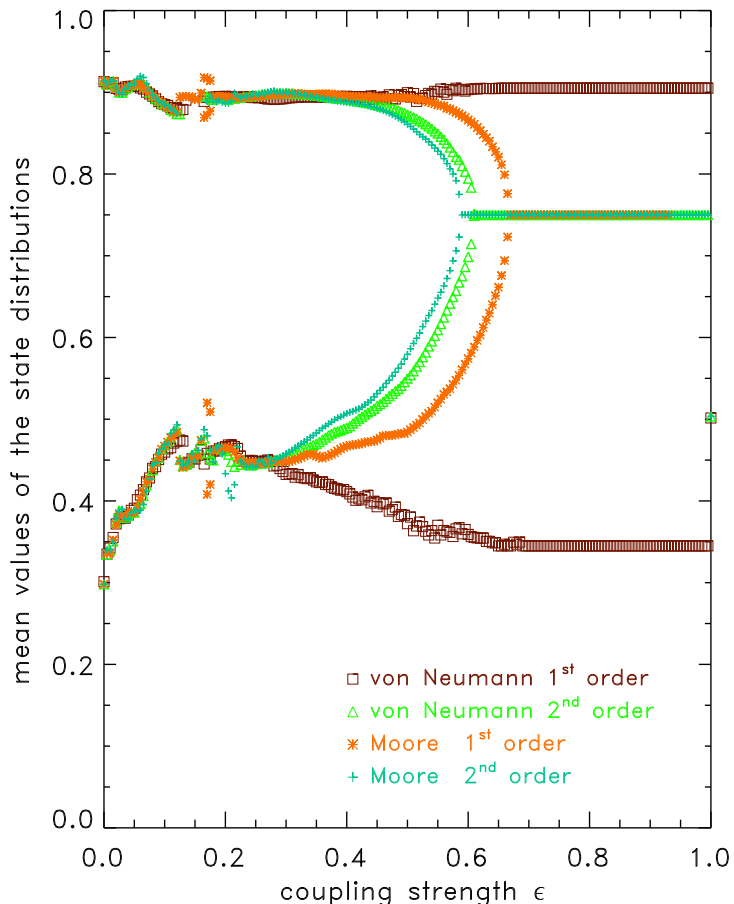


Figure 3: Stability diagram for synchronously updated CMLs with different types of neighborhoods. Mean values of the state distribution right and left of the unstable fixed point at 0.75, averaged over ten sets of random initial conditions, are plotted versus the coupling strength ϵ . The control parameter of the logistic map is set at $r = 4$, and the number of iterations is 10000.

point at 0.75) can be stabilized due to the influence of neighborhoods in coupled map lattices under synchronous updating. Such stabilization is observed for both homogeneous and inhomogeneous perturbations. The only exception found to this rule is a von Neumann neighborhood of order 1 which fails to provide stabilization. Considering higher order neighborhoods of different kinds provides a substantial extension of the observations by Mehta & Sinha [2000] whose studies of synchronous updating were restricted to von Neumann neighborhoods of order 1.

2.2 Asynchronous Updating

For an asynchronous updating procedure, the updating sequence is crucial and should be adapted to the situation which is modeled by the implemented CML. In cases which can be considered more or less spatially homogeneous, a random

selection of the updating sequence is naturally plausible. In the particular case of neurobiological applications, i.e. neural networks, other sequencing mechanisms may be preferable. For instance, it might be appropriate to use a value-dependent asynchronous update (similar to Hopfield [1982]), in which cells with higher values are updated first.

For *random* asynchronous updates, Figs. 4 and 5 show two histograms for the distribution of state values after 10000 iteration steps for a von Neumann neighborhood of order 1 and a Moore neighborhood of order 1, for coupling strengths $\epsilon = 0.47$ (Figs. 4a, 5a) and $\epsilon = 0.57$ (Figs. 4b, 5b). Figs. 4a and 5a show the overall state distribution of the CML. (For a linear update, using the linear sequence of cells as it is given by the structure of the (2D) lattice, there are two peaks right and left of the unstable fixed point at 0.75, indicating oscillatory behavior.) By contrast, Figs. 4b and 5b show that the entire CML is stabilized at the unstable fixed point at 0.75 at each cell for both types of neighborhood.

Figure 6 shows the stability diagram for random asynchronous updating. Stabilization at the unstable fixed point sets in precisely at $\epsilon = 0.5$, beyond which all cells stay at the value 0.75 of the unstable fixed point. (At $\epsilon = 1.0$, this changes to 0.5, the mean value of the distribution of initial state values; compare Fig. 3.) As for synchronous updating, this behavior occurs for both homogeneous and inhomogeneous perturbations. Other than for synchronous updating, the onset of stabilization is independent of the chosen neighborhood. The behavior of the stability curves for $\epsilon < 0.5$ shows small variations for different neighborhood types.

It should be noted here that a *linear* asynchronous updating procedure, leads to the same stability diagram as random asynchronous updating. In this respect, linear updating can be considered as a special case of random updating.

This is not the case for *value-dependent* asynchronous updating, where the updating sequence is determined by the distribution of state values in the preceding time step. As an example, this is demonstrated for the case in which the updating sequence corresponds to the sequence of decreasing state values. i.e. the site with the highest value is updated first etc. In Fig. 7, histograms for the distribution of state values after 10000 iteration steps for such a value-dependent asynchronous updating are presented for coupling strength $\epsilon = 0.47$, (a) for a von Neumann neighborhood of order 1 and (b) for a Moore neighborhood of order 1. For $\epsilon = 0.57$ (and other values of $\epsilon > 0.5$) the distribution of state values looks precisely as for random asynchronous updating in Figs. 4b and 5b.

Fig. 8 shows the stability diagram for value-dependent asynchronous updating. Its overall appearance is similar to Fig. 6. However, the lower branch shows a slight difference in the range $0.4 < \epsilon < 0.5$. It reflects the fact that mean values of the state distribution for states smaller than x_c , the value of the unstable fixed point, tend to approach that value faster than those greater than x_c . Another difference is that the mean value for $\epsilon = 1$ is approximately 0.3 rather than 0.5. This reflects the fact that, as a consequence of the value dependent updating, higher values in the map are more often reduced than small values are increased, thus leading to a lowered mean for perfect coupling.

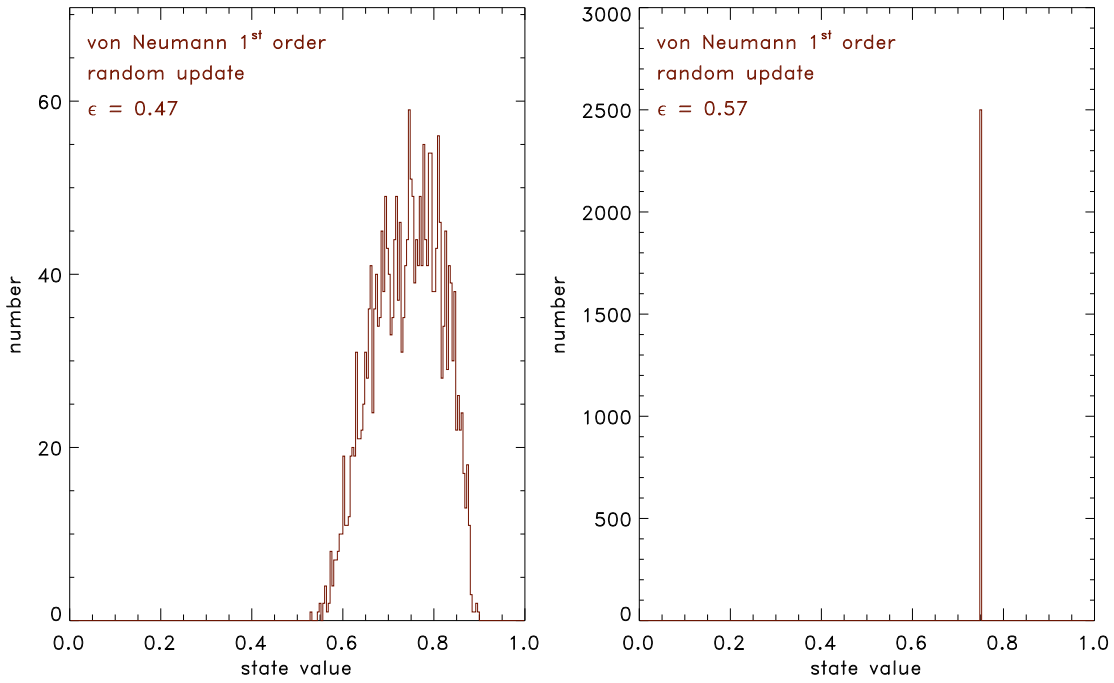


Figure 4: State histograms for random asynchronous updating of CMLs with a von Neumann neighborhood of order 1 for coupling strengths (a) $\epsilon = 0.47$ (left) and (b) $\epsilon = 0.57$ (right). The control parameter of the logistic map is set at $r = 4$, and the number of iterations is 10000.

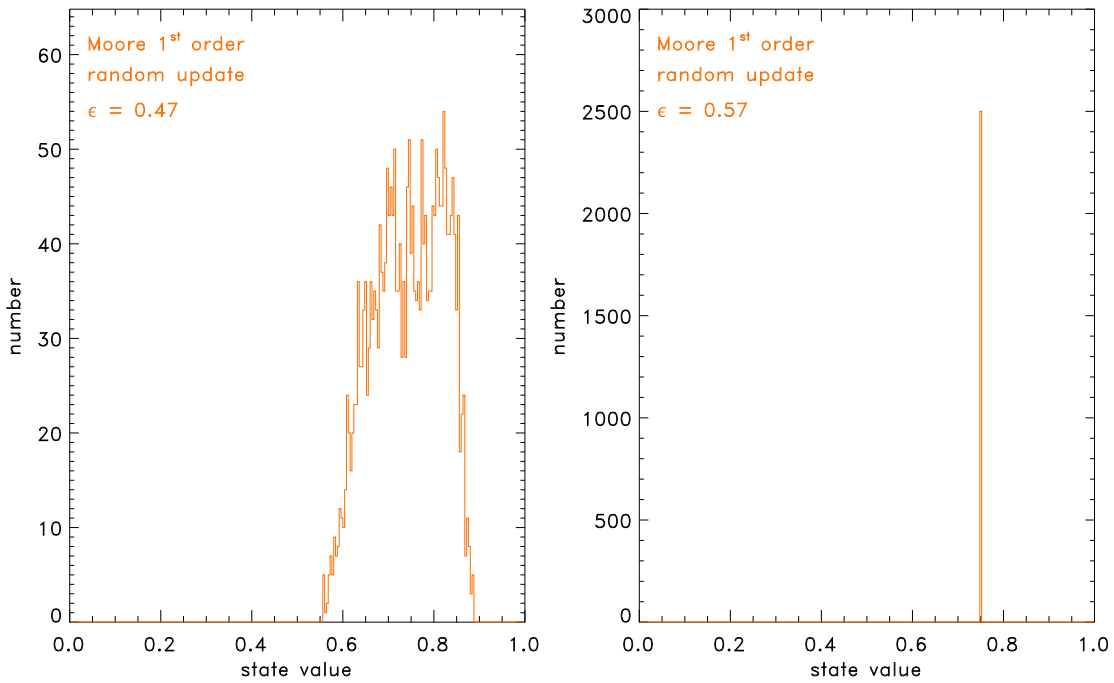


Figure 5: State histograms for random asynchronous updating of CMLs with a Moore neighborhood of order 1 for coupling strengths (a) $\epsilon = 0.47$ (left) and (b) $\epsilon = 0.57$ (right). The control parameter of the logistic map is set at $r = 4$, and the number of iterations is 10000.

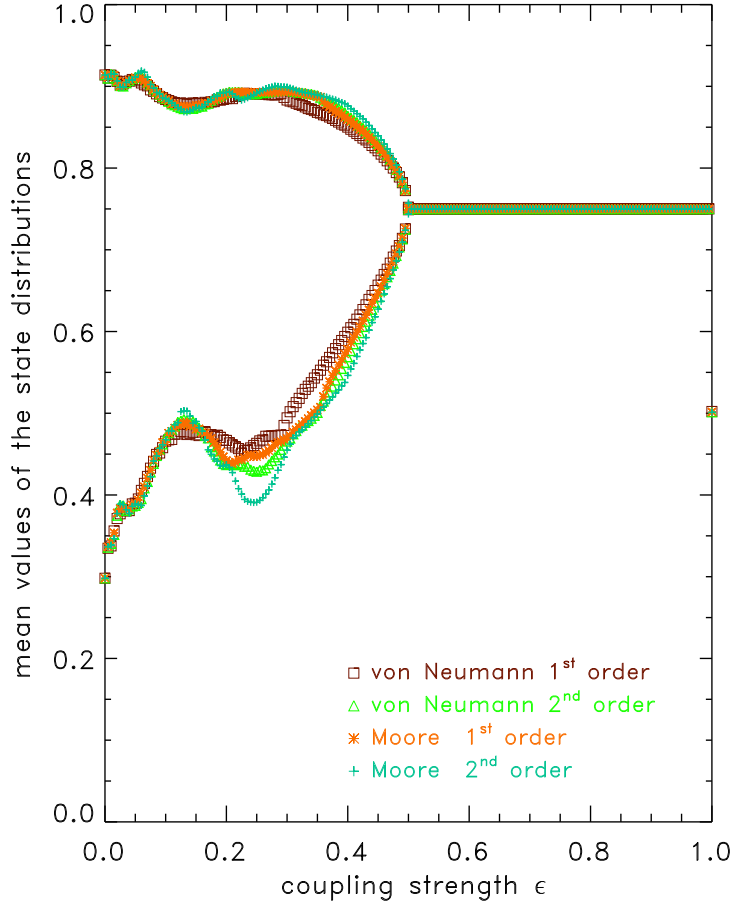


Figure 6: Stability diagram for CMLs with random asynchronous updating for different types of neighborhoods. Mean values of the state distribution right and left of the unstable fixed point at 0.75, averaged over ten sets of random initial conditions, are plotted versus the coupling strength ϵ . The control parameter of the logistic map is set at $r = 4$, and the number of iterations is 10000.

3 Analytical Conditions for Stabilization

To some extent it is possible to understand the stabilization behavior of local unstable behavior of CMLs analytically. In the first term at the rhs of Eq. (1), one may consider $r_{\text{eff}} = (1 - \epsilon)r$ as an “effective” control parameter including the influence of coupling among cells. Then, the maximum of the resulting “effective” logistic map is lowered from $r/4$ to $r_{\text{eff}}/4$, thus leading to a vertically squeezed version of the original map. For this squeezed map, the critical point is $\frac{r_{\text{eff}}-1}{r_{\text{eff}}}$, which is different from the original critical point unless $\epsilon = 0$.

The original critical point can be re-established, if the squeezed map is shifted upward until it intersects the line $x_{n+1} = x_n$ at the critical point $x_c = \frac{r-1}{r}$. Now, the absolute value of the derivative of the squeezed-and-shifted map at x_c is clearly smaller than that of the original map. In particular, its absolute value is smaller

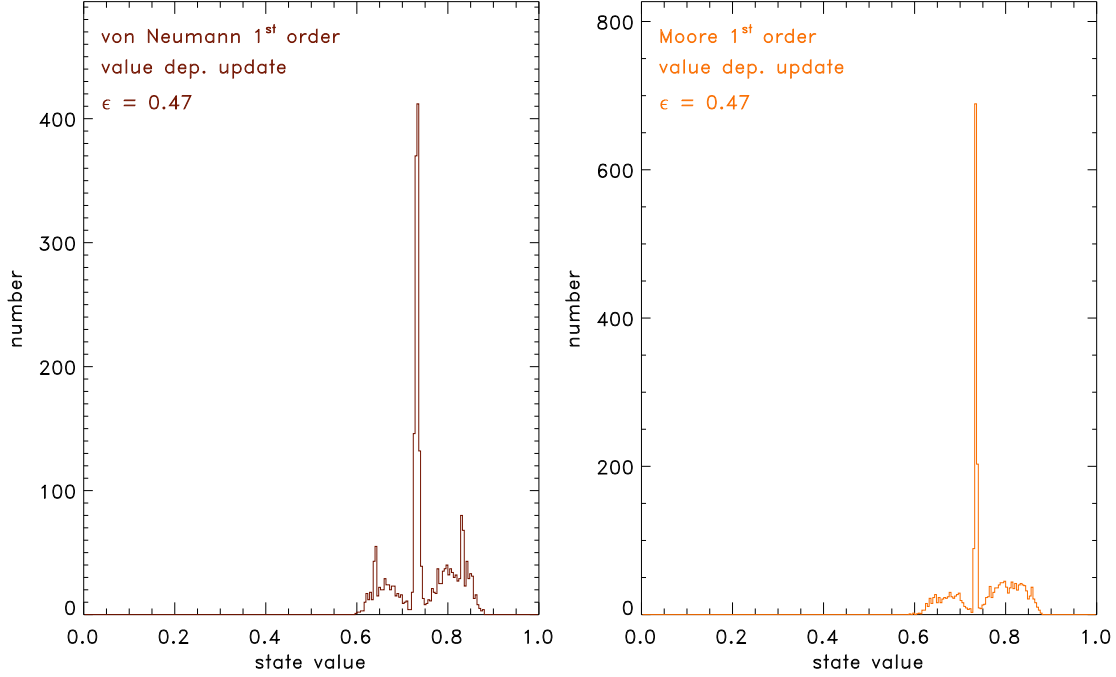


Figure 7: State histograms for value-dependent asynchronous updating of CMLs with (a) von Neumann neighborhood (left) and (b) Moore neighborhood (right) of order 1 for coupling strength $\epsilon = 0.47$. The state histogram for $\epsilon = 0.57$ is identical with that of Figs. 4b and 5b. The control parameter of the logistic map is set at $r = 4$, and the number of iterations is 10000.

than 1 if ϵ is large enough, such that the fixed point becomes stable. Figure 9 illustrates this argument.

The unstable fixed point of the logistic map is stabilized if the distance d between the original logistic map at x_c and the squeezed map at the same value is compensated by the shift due to the neighborhood term in Eq. (1). The distance d (cf. Fig. 9) is given by:

$$d = x_c - f_{\text{squeezed}}(x_c) \quad (2)$$

$$= x_c - rx_c(1 - \epsilon)(1 - x_c) \quad (3)$$

For stabilization, this distance must be equal to the second term in Eq. (1):

$$d = \frac{\epsilon}{N} \sum_{k=1}^N x_k \quad (4)$$

Combining Eqs. (3) and (4) yields:

$$\frac{1}{N} \sum_{k=1}^N x_k = \frac{1}{\epsilon} x_c [1 - r(1 - \epsilon)(1 - x_c)] \quad (5)$$

$$= x_c \quad (6)$$

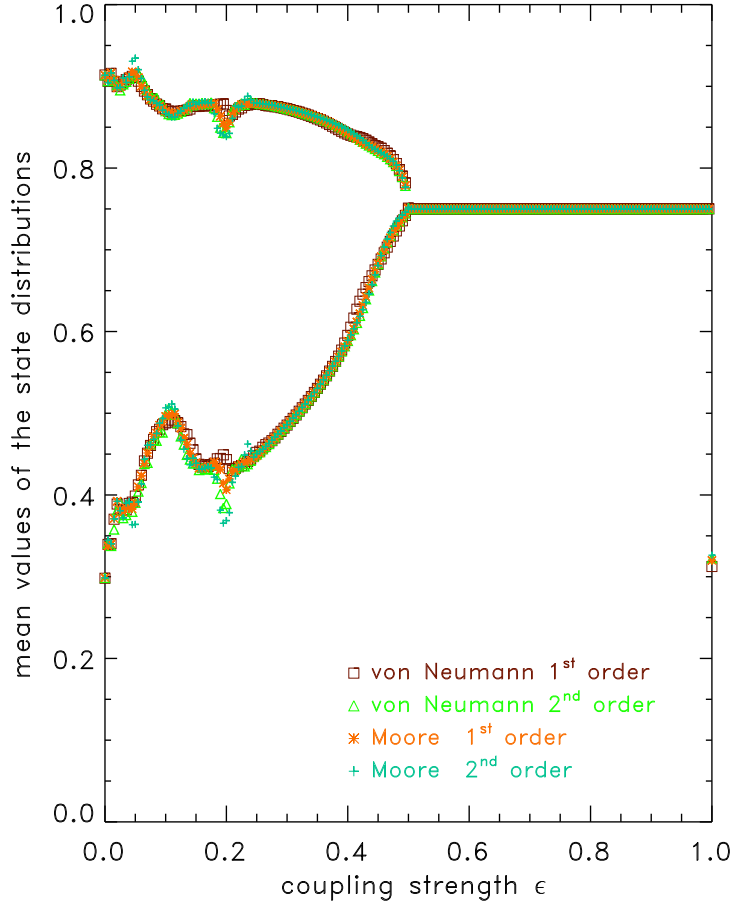


Figure 8: Stability diagram for CMLs with value-dependent asynchronous updating for different types of neighborhoods. Mean values of the state distribution right and left of the unstable fixed point at 0.75, averaged over ten sets of random initial conditions, are plotted versus the coupling strength ϵ . The control parameter of the logistic map is set at $r = 4$, and the number of iterations is 10000.

since some arithmetic shows that:

$$[1 - r(1 - \epsilon)(1 - x_c)] = \epsilon \quad (7)$$

Thus, a first necessary condition for stabilization is that the mean of the state values in all neighborhood cells is exactly the critical value x_c . The distance $d = \epsilon x_c$ itself is independent of the size N of the neighborhood.

The values of ϵ and r which provide stabilization cannot be determined from the derived condition. This means that the quantitative dependence of the stabilization on these parameters cannot be inferred from Eq. (6). Of course, we know that $r > 3$ is required for an unstable fixed point at $\frac{r-1}{r}$. Moreover, it is evident from the numerical results presented in Sec. 2 that ϵ plays a crucial role for stabilization.

The value of ϵ required to make the derivative of the squeezed-and-shifted map equal to -1 at the critical point x_c , thus leading to stabilization, can be obtained

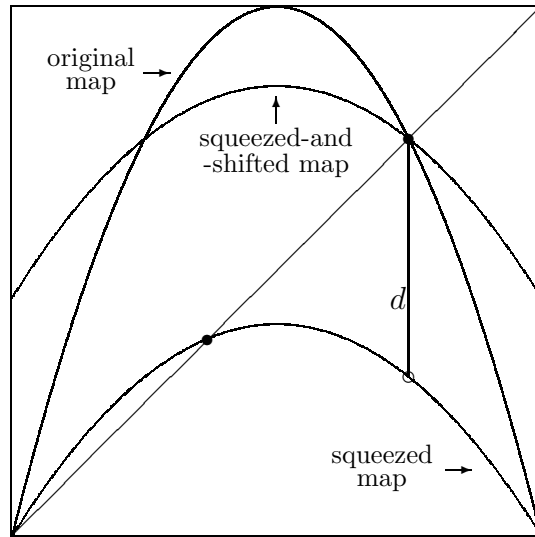


Figure 9: Schematic illustration of the squeeze-and-shift procedure explained in the text. The unstable fixed point of the original logistic map and the stable fixed point of the squeezed map are represented as filled dots; the empty dot indicates the value of the squeezed map at the unstable fixed point of the original map. In order to match the unstable fixed point of the original map, the squeezed map has to be shifted by the distance d .

from the derivative of the squeezed map at x_c :

$$f'(x_c) = r_{\text{eff}}(1 - 2x_c) \quad (8)$$

Setting $f'(x_c) = -1$ yields

$$\epsilon_{lb} = 1 - \frac{1}{r-2} \quad (9)$$

as the lower bound for the coupling strength ϵ_c of stabilization onset. This is a second necessary condition for the global stabilization of an unstable local fixed point. It expresses the fact that the coupling among lattice cells leads to stable behavior as reflected by the squeezed map in Fig. 9, so that the unstable fixed point at individual cells becomes inefficacious. This explains why the stabilization does not depend on whether the perturbation is homogeneous or inhomogeneous, as observed in Secs. 2.1 and 2.2.

For $r = 4$, it follows that $\epsilon_c \geq 0.5$. As can be seen in Figs. 6 and 8, the onset of stabilization for asynchronous updating at $r = 4$ is precisely at $\epsilon_{lb} = \epsilon_c = 0.5$, irrespective of the type of neighborhood chosen and irrespective of the way in which the updating sequence is determined. For $r = 3$, $\epsilon_{lb} = \epsilon_c = 0$ since the fixed point at $\frac{r-1}{r}$ becomes a stable fixed point. Figure 10 shows the functional dependence of ϵ_{lb} on r according to Eq. (9) together with some values of ϵ_c obtained from numerical runs for random asynchronous updating with different values of r . The numerical results ϵ_c match their lower bound ϵ_{lb} perfectly well.

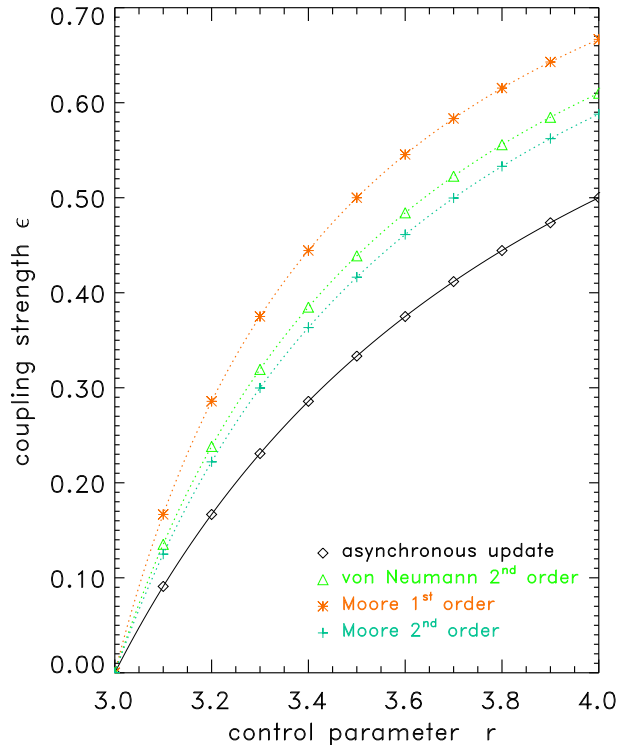


Figure 10: Coupling strength for stabilization onset, ϵ_c , and its lower bound, ϵ_{lb} , as a function of r , $3 \leq r \leq 4$. The solid curve for ϵ_{lb} is obtained from Eq. (9). The individual values along the curve are numerical results of $\epsilon_c = \epsilon_{lb}$ for random asynchronous updating. Values above the theoretical curve represent $\epsilon_c > \epsilon_{lb}$ for synchronous updating with different neighborhoods. The dotted curves represent correspondingly rescaled versions of Eq. (9).

For synchronous updating (cf. Fig. 3), the onset of stabilization (except for a von Neumann neighborhood of order 1) satisfies the lower bound according to Eq. (9) as well. However, the value ϵ_c of stabilization onset is strictly greater than ϵ_{lb} and depends additionally on the neighborhood. This can also be seen in Fig. 10 where ϵ_c is plotted for different kinds of neighborhood. In order to describe the corresponding behavior analytically (dotted lines in Fig. 10), r in Eq. (9) has to be properly rescaled in a way which depends on the size and topology of the neighborhood.

4 Summary and Perspectives

The behavior of two-dimensional lattices of coupled logistic maps with different coupling ϵ , different types of neighborhoods and different updating rules has been studied at and around the unstable fixed point of individual maps. Moore and von Neumann neighborhoods up to second order as well as synchronous and asynchronous updating rules have been considered. It has been found that locally un-

stable behavior of individual maps is stabilized due to the influence of global lattice interactions for particular parameter ranges. The key point of this stabilization is that it operates inherently, i.e. without any need for external adjustment or control.

For synchronous updating, where all sites of the lattice are updated simultaneously, stabilization has been observed for all types of neighborhood with the exception of a von Neumann neighborhood of first order. The onset value ϵ_c for stabilization depends on the type of neighborhood and, of course, on the control parameter r of the logistic map.

For asynchronous updating the sites of the lattice are updated sequentially. This can be straightforwardly implemented in terms of a randomized sequence (or, somewhat more artificially, linearly with respect to the structure of the lattice). Another option is a value-dependent updating procedure, where the updating sequence is determined by the sequence of ordered state values. In both cases, stabilization is always achieved. The coupling strength ϵ_c for its onset depends on r , but not on the type of neighborhood.

Two conditions for stabilization have been derived analytically. The first one states that the sum of the values in all N neighborhood cells must be equal to N times the critical value of the map in order to achieve stabilization. The second condition provides a lower bound for the coupling strength ϵ_c required for stabilization onset. This lower bound is precisely the onset value itself in case of asynchronous updating, but not in case of synchronous updating.

More complicated behavior of coupled map lattices can easily be generated by more complicated lattice features. For instance, first pilot studies combining random and value-dependent asynchronous updating have shown situations in which an onset of stabilization at some ϵ is observed, but the lattice destabilizes again with increasing coupling strength.

The reported results have been obtained for homogeneous and time-independent coupling. Relaxing these conditions leads to plastic networks as recently investigated by Ito & Kaneko [2000, 2002]. Another important novel direction of research concerns so-called scale-free networks (Albert & Barabasi [2002]), where the number of edges, which a node in the network has, is not Poisson distributed (as in a standard random graph) but shows power-law behavior.

5 References

- Albert, R., & Barabasi, A.-L. [2002]: “Statistical mechanics of complex networks”, *Reviews of Modern Physics* **74**, 47–97.
- Atay, F., Jost, J., & Wende, A. [2004]: “Delays, connection topology, and synchronization of coupled chaotic maps”, lanl preprints cond-mat/0312177.
- Atmanspacher, H. [1992]: “Categorical and acategorical representation of knowledge”, *Cognitive Systems* **3**, 259–288.

- Atmanspacher, H., & Wiedenmann, G. [1999]: “Some basic problems with complex systems”, in *Large Scale Systems: Theory and Applications*, ed. by N.T. Kousoulas and P. Groumpos, Elsevier, Amsterdam, pp. 1059–1066.
- Hopfield, J.J. [1982]: “Neural networks and physical systems with emergent collective computational abilities”, *Proceedings of the National Academy of Sciences of the USA* **79**, 2554–2558.
- Ito, J., & Kaneko, K. [2000]: “Self-organized hierarchical structure in a plastic network of chaotic units”, *Neural Networks* **13**, 275–281.
- Ito, J., & Kaneko, K. [2002]: “Spontaneous structure formation in a network of chaotic units with variable connection strength”, *Physical Review Letters* **88**, 028701.
- Kaneko, K., ed. [1993]: *Theory and Applications of Coupled Map Lattices*, Wiley, New York.
- Kaneko, K., & Tsuda, I. [2000]: *Complex Systems: Chaos and Beyond*, Springer, Berlin.
- Kornmeier, J., Bach, M., & Atmanspacher, H. [2004]: “Correlates of perceptive instabilities in event-related potentials”, *International Journal of Bifurcations and Chaos* **14**, 727–736.
- Kuhn, A., Aertsen, A., & Rotter, S. [2004]: “Neuronal integration of synaptic input in the fluctuation-driven regime”, *Journal of Neuroscience* **24**, 2345–2356.
- Li, C., Li, S., Liao, X., & Yu, J. [2004]: “Synchronization in coupled map lattices with small-world delayed interactions”, *Physica A* **335**, 365–370.
- Lumer, E.D., & Nicolis, G. [1994]: “Synchronous versus asynchronous dynamics in spatially distributed systems”, *Physica D* **71**, 440–452.
- Mackey, M., & Milton, J. [1995]: “Asymptotic stability of densities in coupled map lattices”, *Physica D* **80**, 1–17.
- Marcq, P., Chaté, H., & Manneville, P. [1997]: “Universality in Ising-like phase transitions of lattices of coupled chaotic maps”, *Physical Review E* **55**, 2606–2627.
- Masoller, C., Marti, A.C., & Zanette, D.H. [2003]: “Synchronization in an array of globally coupled maps with delayed interactions”, *Physica A* **325**, 186–191.
- Mehta, M., & Sinha, S. [2000]: “Asynchronous updating of coupled maps leads to synchronization”, *CHAOS* **10**, 350–358.
- Ott, E., Grebogi, C., & Yorke, J.A. [1990]: “Controlling chaos”, *Physical Review Letters* **64**, 1196–1199.

Rolf, J., Bohr, T., & Jensen, M.H. [1998]: “Directed percolation universality in asynchronous evolution of spatiotemporal intermittency”, *Physical Review E* **57**, R2503–R2506.

Turing, A. [1952]: “The chemical basis of morphogenesis”, *Transactions of the Royal Society London, Series B* **237**, 37–72.